THE AMERICAN SOCIETY OF MECHANICAL ENGINEERS
345 E. 47th St., New York, N.Y. 10017

96-GT-476

LDA STUDY OF THE FLOW DEVELOPMENT THROUGH AN ORTHOGONALLY ROTATING U-BEND OF STRONG CURVATURE AND RIB ROUGHENED WALLS.

H. Iacovides, D.C. Jackson, H. Ji, G. Kelemenis, B.E. Launder and K. Nikas
Department of Mechanical Engineering, UMIST, P O Box 88, Manchester M60 1QD, UK

ABSTRACT

This paper reports laser Doppler anemometry (LDA) and wall pressure measurements of turbulent flow in a square-sectioned, rotating U-bend typical of coolant passages employed in modern gas turbine blades. In the upstream and downstream tangents, the pressure and suction (inner and outer) surfaces are roughened with discrete square-sectioned ribs in a staggered arrangement for a rib-height to duct-diameter ratio of 0.1. Three cases have been examined at a passage Reynolds number of 10^5: a stationary case; a case of positive rotation (the pressure side coinciding with the outer side of the U-bend) at a rotation number ($Ro=\Omega D/U_m$) of 0.2; and a case of negative rotation at Ro=-0.2. Measurements have been obtained along the symmetry plane of the duct. In the upstream section, the separation bubble behind each rib is about 2.5 rib-heights long. Rotation displaces the high momentum fluid towards the pressure side, enhances turbulence along the pressure side and suppresses turbulence along the suction side. The introduction of ribs in the straight sections reduces the size of the separation bubble along the inner wall of the U-bend, by raising turbulence levels at the bend entry; it also causes the formation of an additional separation bubble over the first rib interval along the outer wall, downstream of the bend exit. Rotation also modifies the mean flow development within the U-bend, with negative rotation speeding up the flow along the inner wall and causing a wider inner-wall separation bubble at exit. Turbulence levels within the bend are generally increased by rotation and, over the first two diameters downstream of the bend, negative rotation increases turbulence while positive rotation on the whole has the opposite effect.

NOMENCLATURE

C_p	pressure coefficient ($=(P-P_{ref}) / (0.5\rho U_m^2)$)
D	duct hydraulic diameter
h	rib height
P	rib pitch
R_c	bend mean curvature
Re	flow Reynolds number ($\rho U_m D/\nu$)
Ro	Rotation number ($=\Omega D/ U_m$)
U_m	bulk velocity
U_x	cross-duct velocity
U_z	streamwise velocity
x	cross-duct direction
z	streamwise direction
ν	kinematic viscosity
Ω	angular velocity of rotating duct

1. INTRODUCTION

Flow and heat transfer in U-bends of strong curvature is of direct relevance to the internal cooling of gas-turbine blades. In modern gas-turbines, relatively cool air, extracted from the compressor stages of the engine, is circulated through internal cooling passages inside the turbine rotor blades, in order to maintain the operating temperature of the blades at safe levels. Flow and heat transfer inside these cooling channels are affected by the presence of sharp U-bends, the rotation of the blades giving rise to Coriolis and rotational buoyancy forces, and the presence of heat-transfer-enhancing ribs.

In three-dimensional flows through either curved or rotating passages, both the Coriolis force and curvature induce strong secondary motions (See, for example, Moon, 1964,; Taylor et

Presented at the International Gas Turbine and Aeroengine Congress & Exhibition
Birmingham, UK — June 10-13, 1996
This paper has been accepted for publication in the Transactions of the ASME
Discussion of it will be accepted at ASME Headquarters until September 30, 1996

al, 1982; Chang et al, 1983). In blade cooling passages, space constraints dictate that the U-bend must be so tight that flow separation occurs downstream of the bend and also possibly at the bend entry. The flow thus becomes considerably more complex, even in the absence of ribs and rotation. The combined effects of strong curvature and orthogonal rotation have been examined in our earlier experimental study (Cheah et al, 1994), in which detailed LDA data were collected for flow through a U-bend of square cross-section and of curvature ratio (R_c/D) of 0.65 that was either stationary or rotating about an axis parallel to the axis of curvature. In that study the inlet and exit tangent ducts were smooth and the rotation and bend-curvature axes were parallel. While this configuration differs from gas-turbine practice it has the advantage that, in principle, the flow is symmetric about the plane orthogonal to the rotation axis passing through the centre plane of the duct. Moreover, it is a condition for which convective heat transfer data have already been obtained (Wagner et al, 1989).

Here the results of a subsequent investigation are reported in which the effects of discrete roughness elements have been included. As shown in Figure 1, square ribs have been added to the straight sections of the square-sectioned U-bend, in a staggered arrangement along the inner and outer walls. The objective is to generate detailed mean and turbulent flow data that reveal how the ribs modify the flow development within the U-bend under both stationary and rotating conditions. Such data should not only improve our understanding of blade cooling flows, but would also provide challenging test cases for further assessment of turbulence models used in the computation of blade-cooling flows.

2. EXPERIMENTAL APPARATUS AND PROCEDURE

As described in (Cheah et al, 1994), the rig consists of a motor-driven turntable mounted in a 1.22m diameter water tank. A rib-roughened U-bend of 0.05m square cross-section and of curvature ratio R_c/D=0.65, shown in Figure 1, is mounted on a turntable so that the curvature axis of the duct is parallel to the axis rotation of Fig 2. This mode of rotation was selected because the geometrical plane of symmetry of the U-bend still remains the hydrodynamic plane of symmetry. The inner and outer duct walls of the upstream and downstream sections are artificially roughened using ribs of square cross-section in a staggered arrangement. The ribs are oriented normal to the duct axis. The rib-height-to-duct-diameter ratio h/D is 0.1 and the pitch-to-height ratio, P/h, is 10. The closing side walls of the duct are smooth. The axial throughflow to the test rig is fed into the square duct through a passage that is built into the rotating turntable and the outflow is exhausted into the open water tank. A combination of fine wire-meshes and a honeycomb section are located downstream of the flow entrance to the duct to provide uniform and symmetric flow into the U-bend section. The test section is made of 0.01m thick perspex to facilitate optical access by LDA laser beams.

The rotor/turntable could be driven at any speed up to 250rpm in either direction. A feedback control circuit utilises the input signals from a shaft rotary encoder to control precisely the rotational speed.

The LDA system employed was a TSI two-channel, four-beam fibre-optic system with frequency shifting on both the blue and the green channels. A 4-watt Argon-ion laser was used to power the system and two counter processors (TSI 1980B) were used for signal validation. Subsequent data processing was done through a Zech data acquisition card on a PC. LDA measurements have so far been collected along the duct symmetry plane. A fibre-optic probe, of focal length 0.135m, was mounted in a stationary position above the turntable as seen in Figure 2. The laser beams entered the top wall of the duct, with the LDA measurements being taken as the rotating duct swept across the beams. Simultaneous two-component velocity measurements were collected, with a coincidence window of 20 μs, at several selected radial locations. The position of each data point in the flow was indexed by an incremental rotary encoder mounted on the rotating drive-shaft. Measurements from each discrete angular location were then recorded in separate data bins. The stationary probe was thus able to collect rotating flow data along circumferential lines as shown in Figure 3(a). A 1/8-degree resolution produced 2880 data bins per traverse line. A total of 60,000-80,000 data points was gathered in each traverse. The maximum circumferential length of a data bin was 0.6mm and the average closer to 0.3mm. For the turbulence quantities, data from up to 3 adjacent bins were combined to produce a sufficiently large sample at each angular position. To obtain profiles along straight traverse lines across the duct, 3 circumferential traverses were performed along 3 close radial positions, so as to envelope the required cross-duct line as shown in Figure 3(a). The corresponding straight-line profiles were then obtained through interpolation. Measurements within the U-bend were obtained along eleven equispaced radial traverses shown in Figure 3(b). Bi-linear interpolation was then used to construct profiles along radial lines. For the stationary case manual traverses were carried out.

In addition to the LDA data, wall static pressure measurements were also collected through a series of static

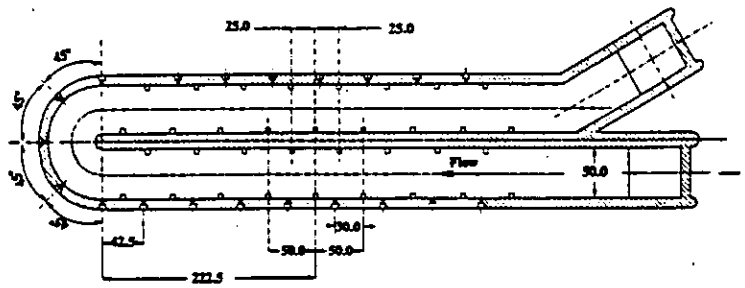

Figure 1. Experimental Model

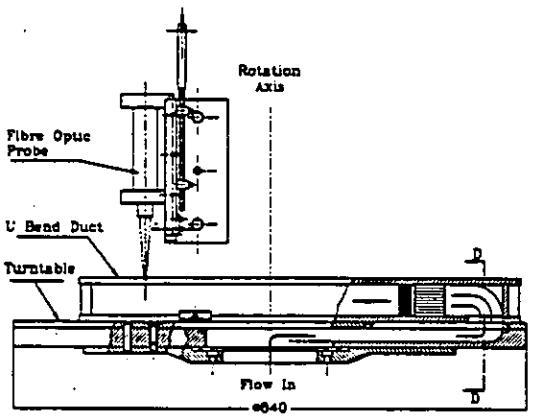

Figure 2. Experimental Apparatus

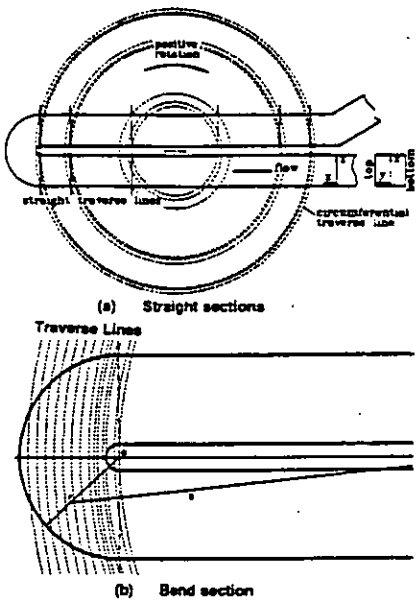

Figure 3. LDA Traverse Paths

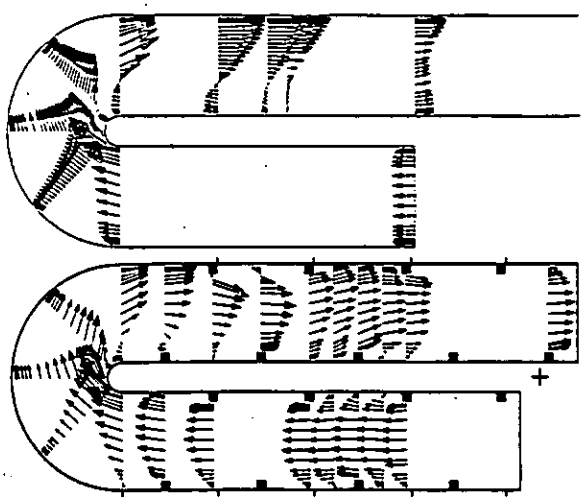

Figure 4. Mean flow comparisons for stationary U-bends.

In addition to the LDA data, wall static pressure measurements were also collected through a series of static pressure taps along the top (flat) wall. The pressure taps were connected to pressure transducers attached to the rotating model and, through slip-rings, the transducer output was transmitted to a data processing PC.

The fluid temperature was maintained at a uniform level to within 0.2° C. The mass flow rate was monitored by an orifice run installed in ducting preceding the U-bend.

The overall estimated uncertainties for the streamwise and cross-duct velocity components U_Z and U_X respectively, and of the corresponding turbulence quantities are:

$$U_Z \leq 0.02U_m \qquad \sqrt{\overline{u_Z^2}} \leq 0.02U_m$$

$$U_X \leq 0.03U_m \qquad \sqrt{\overline{u_X^2}} \leq 0.02U_m$$

$$\overline{u_X u_Z} \leq 0.04U_m^2$$

3. PRESENTATION AND DISCUSSION OF RESULTS

Three cases have been investigated in this study, all for a flow Reynolds number of 100,000: a stationary U-bend, a case for a U-bend rotating positively at Ro=0.2 and one with negative rotation at Ro=-0.2. In all cases traverses have been carried out both within the U-bend and also within the upstream and downstream straight sections. These traverses yielded measurements of the mean velocity components in the streamwise and cross-duct directions, measurements of the corresponding turbulence intensities and shear stress and also measurements of the four triple correlations associated with this plane.

The vector plots of Figure 4 present a comparison between the mean flow development through a stationary U-bend with smooth walls, obtained earlier (Cheah et al, 1994), and the corresponding flow development for the ribbed U-bend, obtained in the present study. Within the straight upstream section, the present measurements show that the flow is fully-developed, with the same flow pattern being repeated over successive rib intervals. The separation bubble downstream of each rib is about 0.25 diameters long, or 2.5 rib heights. The effects of the U-bend appear to extend to only about one hydraulic diameter upstream of the bend entry. There, the adverse pressure gradient along the outer wall extends the length of the separation bubble downstream of the last rib to over 5 rib heights. Thus, in contrast to the smooth wall case, there is now a small region of flow separation along the outer wall at the bend entry. Along the inner wall, the introduction of ribs appears to delay flow separation, which now occurs after the 90° plane. The subsequent separation bubble is not as wide as that formed in the absence of ribs. Reattachment occurs at about one diameter downstream of the bend exit, whereas for the smooth U-bend reattachment occurs at about 2.2 diameters. It is interesting to note that the first downstream rib along the inner wall, 0.45 diameters after the bend exit, is within the separation bubble. Along the outer wall, as in the smooth U-bend, the favourable pressure gradient initially causes a strong flow acceleration at the bend exit. The first downstream rib along the outer wall, 0.95 diameters from the bend exit, consequently poses a greater obstacle to the flow, leading to a large region of flow separation over the first rib interval, which displaces the high momentum fluid towards the duct centre. In contrast (and in consequence), over the second rib interval, there is almost no flow separation along the outer wall. By about six diameters downstream of the bend exit, fully periodic flow conditions are restored.

The effects of rotation on the mean flow, are shown in the vector plots of Figure 5 and the mean velocity profiles of Figure 6. In the upstream section where repeating flow conditions are again in evidence, positive rotation displaces the faster fluid towards the outer wall, which is also the pressure side of the rotating duct, while negative rotation has the opposite effect. This is a consequence of the rotation-induced secondary flow. Rotation also has a noticeable effect on the flow development within the U-bend. As can be more clearly seen in Figure 6, positive rotation leads to a more uniform velocity distribution within the bend, by lowering velocities along the inner side, whereas with negative rotation, the high momentum fluid remains closer to the inner side. These effects are consistent with the rotation effects observed in flow through smooth U-bends, (Cheah et al, 1994). The Coriolis induced secondary motion convects the high momentum fluid towards the pressure side of the rotating duct. Negative rotation increases the width of the inner wall separation bubble over the first downstream rib and, again, positive rotation has the opposite effect. Because with negative rotation the inner side fluid has a higher momentum, it is less able to follow the curvature of the inner wall. As it comes out of the U-bend, the fluid is thus directed to the outer side, leaving a larger separation bubble along the inner wall. The enlarged separation bubble over the first rib interval along the outer wall, is still present with both modes of rotation. The influences of rotation on the mean flow

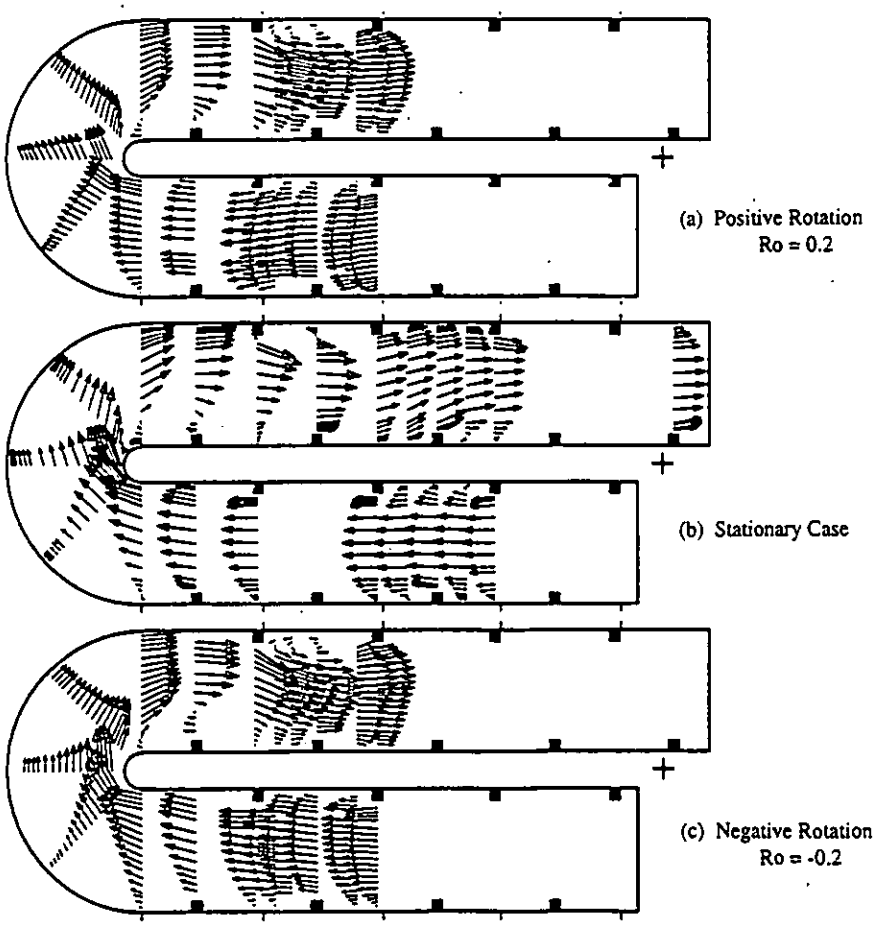

Figure 5. Comparison of mean velocity fields for ribbed U-bend.

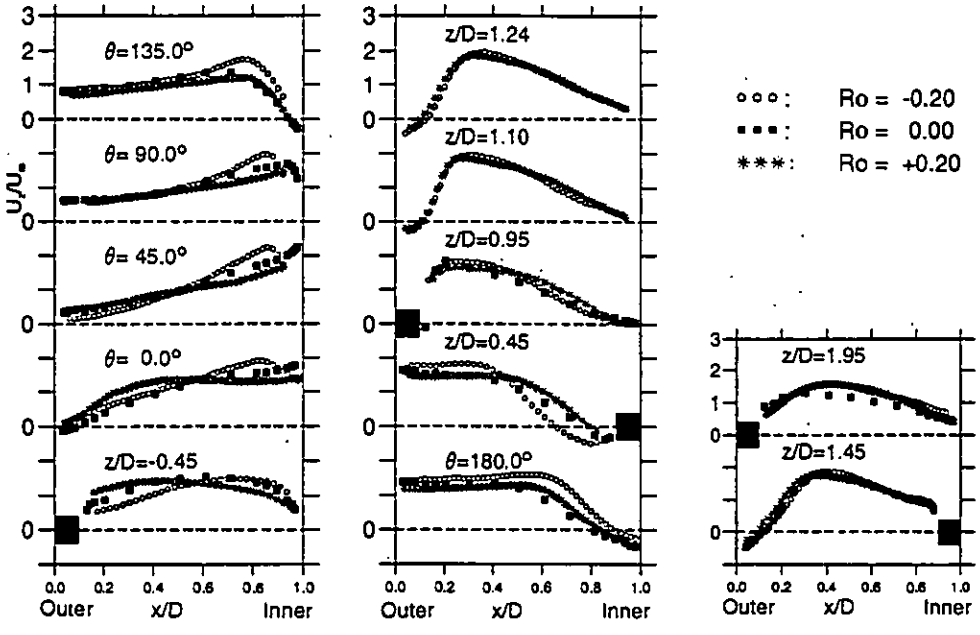

Figure 6. Profiles of streamwise Velocity

development in a rib-roughened U-bend are at least as strong as those observed in flows through similar U-bends with smooth walls.

Figure 7, shows profiles of the turbulent stresses measured within a rib interval which is far enough downstream of the bend for periodic flow conditions to prevail. As expected, the levels of turbulence are considerably higher than those observed in the straight sections of the U-bend with smooth walls (Cheah et al, 1994). Turbulence levels become higher over the ribs, and also in the near-wall regions downstream of the ribs, where the flow is separated. Streamwise turbulence levels are generally higher than the cross-duct levels in the near-wall regions. Rotation appears to increase the streamwise turbulence intensities along the pressure side (which for positive rotation is the outer side and for negative rotation the inner side) of the duct. Moreover, due to the onset of secondary motion, rotation also leads to an overall increase in the levels of the cross-duct turbulence intensities. The effects of rotation on turbulence are also evident in the turbulent shear stress profiles of Figure 7(c). Along the pressure side, rotation increases shear stress levels while, along the suction side, levels are suppressed relative to their stationary duct values.

Figure 8 shows profiles of streamwise turbulence intensities in the vicinity of the U-bend. Because of the ribs in the upstream section, the flow is highly turbulent at the bend entry, especially along the outer wall due to the adverse pressure gradient. These higher turbulence levels at the bend entry are responsible for the delayed flow separation along the inner wall and the smaller subsequent separation bubble. Over the second half of the bend, where a separation bubble is formed along the inner wall, there is a marked increase in near-wall turbulence levels and, as the separation bubble grows further downstream, the high turbulence levels move towards the duct centre. The main characteristic downstream of the U-bend, is the strong rise in turbulence levels along the outer wall over the first rib-interval. This is caused by the large separation bubble formed over this region, shown in Figures 4, 5 and 6. Both positive and negative rotation enhance core turbulence within the U-bend. Downstream of the bend, as also noted in the our earlier study (Cheah et al, 1994), negative rotation generally leads to higher levels of turbulence. The effects of rotation on turbulence within and downstream of the U-bend are not however as strong as those observed in the corresponding study of the smooth U-bend (Cheah et al, 1994). Figure 9 indicates that, in the region immediately downstream of the bend exit, there is a substantial rise in the turbulent shear stress. This increase is more noticeable after the first outer-wall rib. Negative rotation appears generally to augment the turbulent shear stress in the downstream region, whereas positive rotation tends to attenuate it.

Finally Figure 10, shows the variation in static pressure along the top (flat) wall, for both a smooth and a ribbed U-bend. The smooth duct data indicate that in the upstream section, frictional losses are not significantly affected by rotation. For the stationary and positively rotating U-bends there is a small rise in static pressure within the bend whereas, for the case of negative rotation, where as shown in (Cheah et al, 1994) there is flow separation at the bend entry, there is a drop in static pressure within the bend. A strong drop in static pressure occurs at the bend exit, where of course, a large separation bubble is present. This decrease in pressure is greater for the two rotating cases. A partial recovery begins about two diameters after the bend exit for the stationary and negatively rotating U-bends, whereas for positive rotation, where the separation bubble is longer, recovery begins one diameter further downstream. Negative rotation, which increases turbulence levels within and downstream of the bend, also leads to greater loss in static pressure.

For the case of the ribbed U-bend, frictional losses within the straight upstream section are much greater than those in the corresponding smooth sections. In the straight upstream section, where curvature effects are negligible, frictional losses are again not significantly affected by rotation, at least not for Ro values of 0.2. Over the bend entry the pressure rise is least for the stationary case because of the presence of separation at the entry. The decrease in pressure at the bend exit is not as strong as in the smooth U-bend, possibly because the separation bubble along the inner wall is not as large, but the subsequent recovery is also weaker in the ribbed downstream section. The U-bend thus causes a similar pressure loss in the ribbed test model as in the smooth, but there are greater frictional losses in the upstream and downstream ribbed sections. Again negative rotation leads to a greater overall loss in static pressure.

4. CONCLUDING REMARKS

The reported measurements provide insight into the flow structure within a rotating hairpin bend roughened with discrete ribs for a rotation number of 0.20, similar to that encountered in internal cooling passages of gas turbine blades. Comparisons with our recent analogous studies of flow through a smooth U-bend reveal that:

- ◊ In the fully developed sections, away from the bend influence, resistance to streamwise flow arising from the ribs results in the flow pattern and pressure drop

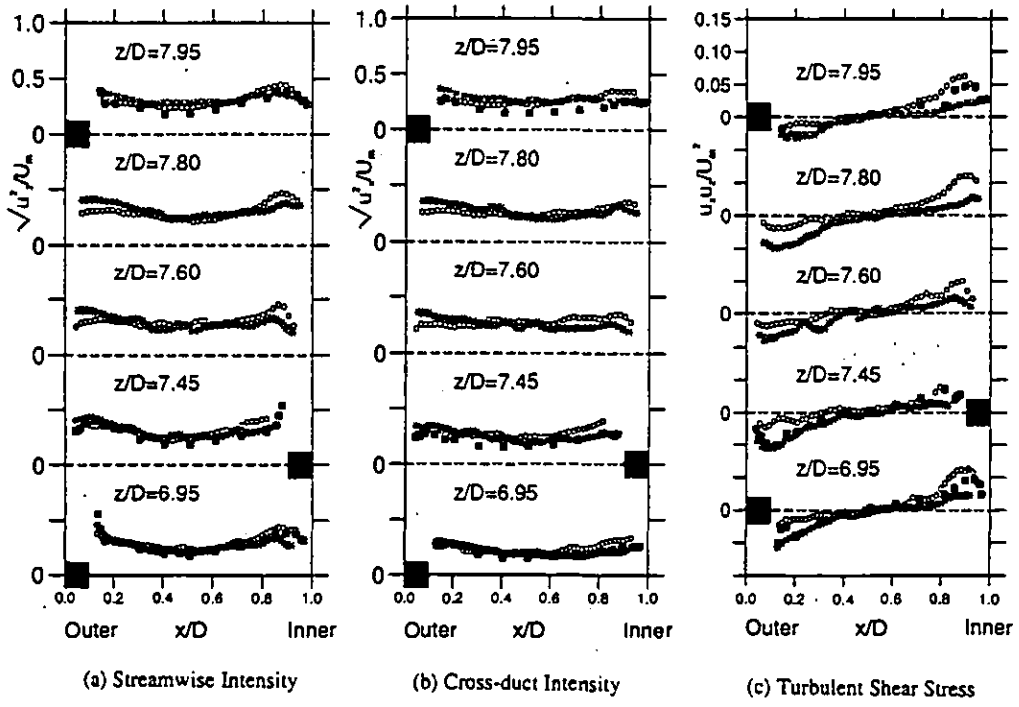

Figure 7. Turbulence profiles for fully developed flow in the straight sections.

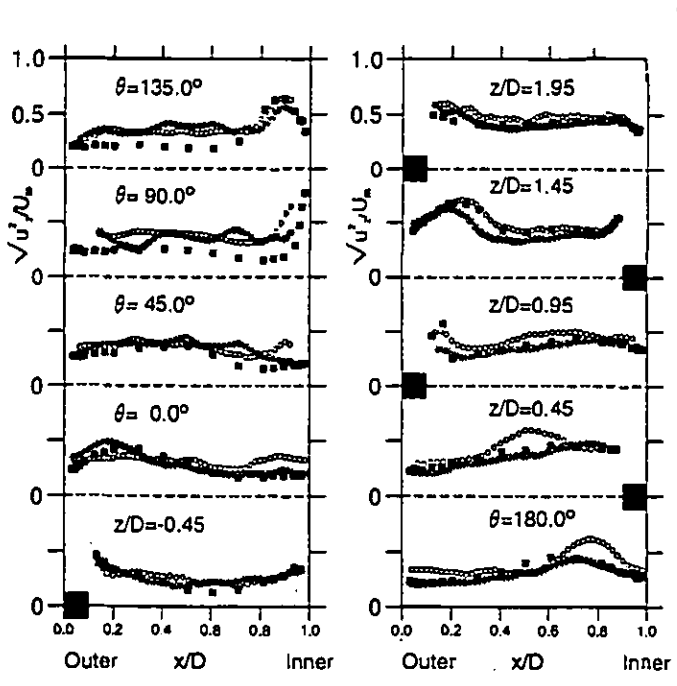

Figure 8. Profiles of streamwise turbulence intensity within and immediately after the U-bend.

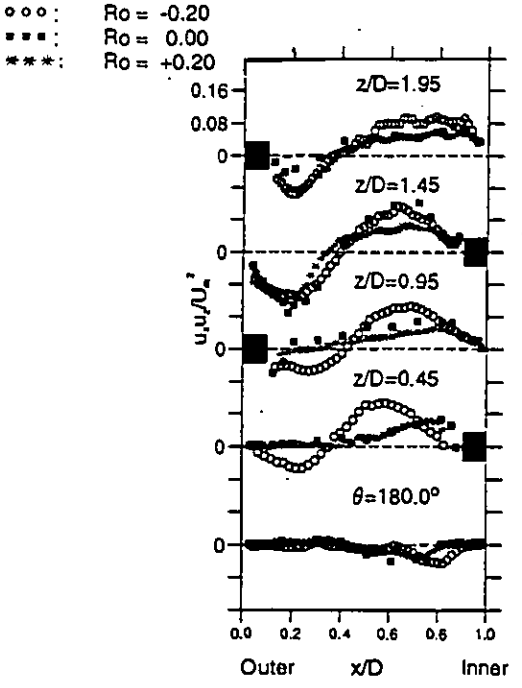

Figure 9. Turbulent Shear Stress profiles immediately after the U-bend.

◊ The ribs also reduce the region of bend influence to about one diameter ahead of and six diameters downstream of the U-bend.

◊ At entry to the bend, the upstream ribbing along the outer-bend wall coupled with the adverse pressure gradient leads to separated or nearly separated flow on this wall; in consequence, the flow near the inner wall is stronger.

◊ Principally because of the much higher turbulence levels with the ribbed wall, separation from the inner wall is delayed somewhat and the separation bubble is thinner than for the smooth duct; nevertheless, the first inner-wall rib downstream of the U-bend actually lies within the separated flow zone.

◊ The flow acceleration at exit near the outer-wall means that the first rib on that surface imposes a greater blockage than elsewhere and a recirculating flow that extends to the next rib.

Further measurements are in progress close to the smooth side walls which will give a more complete picture than the centre-plane measurements reported here. Measurements are also being made with the first downstream rib removed to discern the effects that this has on the flow downstream of and, indeed, within the U-bend. Even the present data should, however, provide a very challenging data set for those wishing to assess the capabilities for their CFD codes for blade cooling applications.

ACKNOWLEDGEMENTS

This research has been supported by ABB (Switzerland), Electricité de France, European Gas Turbines, Rolls-Royce plc and the Defence Research Agency (Pyestock). Outstanding technical assistance has been provided by Mr J Hosker and Mr D Cooper. Authors' names are listed alphabetically.

REFERENCES

Chang S. M., Humphrey J. A. C., and Modavi A., 1983, "Turbulent Flow in a strongly curved U-bend and Downstream Tangent of Square Cross-Section," Physico-Chemical Hydrodynamics, Vol. 4, p.243.

Cheah S. C., Iacovides H., Jackson D. C., Ji H., and Launder B. E., 1994, "LDA investigation of the Flow Development through Rotating U-ducts," ASME Paper 94-GT-226, Int Gas-Turbine and Aero Congress, The Hague.

Moon I. M., 1964, "Effects of Coriolis Force on the Turbulent Boundary Layer in Rotating Fluid Machines," MIT Gas-Turbine Laboratory, Report No. 74.

Moore J., 1967, "Effects of Coriolis on Turbulent Flow in Rotating Rectangular Channels," MIT Gas-Turbine Laboratory, Report No. 89.

Taylor A. M. K. P., Whitelaw J. H., and Yianneskis M. J., 1982, "Curved Ducts with strong secondary Motion: Velocity measurements of developing Laminar and Turbulent Flow," ASME, J Fluids Engrg, Vol. 104, pp. 350-359.

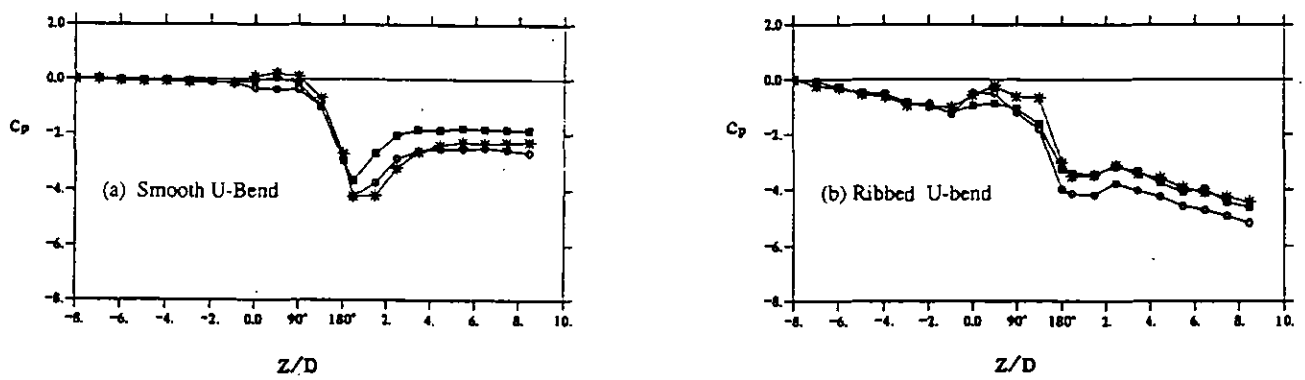

Figure 10. Static pressure variation along the top (flat) wall.
■ : Stationary U-bend, * : Ro = + 0.2, o : Ro = - 0.2